JACS
JOURNAL OF THE AMERICAN CHEMICAL SOCIETY
Communication
pubs.acs.org/JACS

The Least Stable Isomer of BN Naphthalene: Toward Predictive Trends for the Optoelectronic Properties of BN Acenes

Zhiqiang Liu,[†,∥,⊥] Jacob S. A. Ishibashi,[†,∥] Clovis Darrigan,[‡] Alain Dargelos,[‡] Anna Chrostowska,*[,‡] Bo Li,[†] Monica Vasiliu,[§] David A. Dixon,[§] and Shih-Yuan Liu*[,†]

[†]Department of Chemistry, Merkert Chemistry Center, Boston College, Chestnut Hill, Massachusetts 02467, United States
[‡]Institut des Sciences Analytiques et de Physico-Chimie pour l'Environnement et les Matériaux, UMR CNRS 5254, Université de Pau et des Pays de l'Adour, Pau, France
[§]Department of Chemistry, The University of Alabama, Tuscaloosa, Alabama 35487, United States

Supporting Information

ABSTRACT: The least stable isomer of the parental BN naphthalene series has been synthesized in a simple four-step sequence. Its experimental electronic structure characterization via UV-PES, cyclic voltammetry, and UV−vis spectroscopy in direct comparison with three other known BN naphthalene isomers has established two guiding principles for predicting the electronic structures of BN acene compounds: (1) Orientational BN isomers have similar HOMO−LUMO gaps. (2) For each pair of orientational BN isomers, the more thermodynamically stable compound has the lower HOMO energy. Furthermore, we demonstrate that BN/CC isosterism in the context of **BN-9,1-Naph** can impact crystal packing to favor a cofacial π-stack motif.

BN/CC isosterism, i.e., the replacement of a CC unit with a BN unit, has emerged as an effective strategy to expand the chemical space of organic molecules.[1] In particular, the application of BN/CC isosterism to polycyclic aromatic hydrocarbons (PAHs) has attracted interest due to its potential to create new materials for organic optoelectronic devices.[2] While many BN-perturbed analogues of PAHs now exist,[3] the development of a fundamental understanding of the consequences of BN/CC replacement on the electronic structure has been underexplored. For instance, a systematic investigation into how the position and orientation of the BN bond pair influence frontier orbital energetics has not been conducted.[4] The slow progress in this area is due in part to the lack of available synthetic methods to access the various permutations of possible BN isosteres of a PAH motif.[5] We have been employing a bottom-up synthetic approach to investigate BN isosteres of monocylic[6] and polycylic[7] aromatic hydrocarbons. In particular, we have focused on the unsubstituted ("parental") BN isosteres of PAHs in order to characterize their electronic structure that is untarnished by substituent effects.[7,8] Among the PAHs, the naphthalene framework stands out as the most simple PAH motif to apply a systematic BN/CC isosterism investigation. For naphthalene, six permutations exist to replace a C=C unit with a BN bond unit (Figure 1).

Of these six isomers, only three have been isolated to date. Dewar first reported two of these parental BN isosteres of naphthalene, **BN-1,2-Naph**[9] and **BN-9,10-Naph**,[10] in 1959 and 1964, respectively. Recently, we described the synthesis of the **BN-1,9-Naph** isomer.[8b] While substituted derivatives of **BN-2,1-Naph** have been reported by Cui,[11] the parental **BN-2,1-Naph** isomer has not been synthesized. To the best of our knowledge, **BN-2,3-Naph** has also not been disclosed. Of the 6 BN isosteres of naphthalene, **BN-9,1-Naph** is the least thermodynamically stable (Figure 1). Undaunted by this challenge, we targeted this missing isomer because in conjunction with **BN-1,9-Naph**, the effect of orientation of the BN bond placement on the electronic structure could be elucidated.

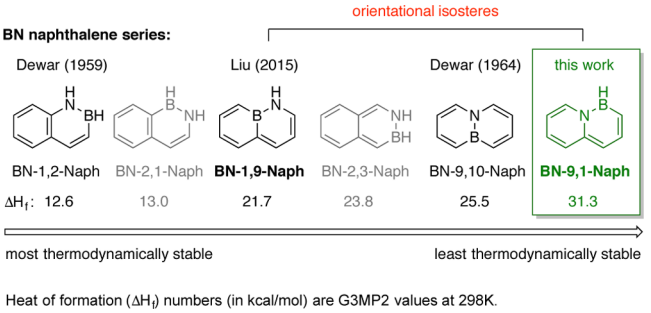

Figure 1. Parental BN isosteres of naphthalene bearing one BN unit. Compounds in gray have not been reported.

In this communication, we describe a simple four-step synthesis of **BN-9,1-Naph**. The experimental characterization of the electronic structure (UV-PES, UV−vis, electrochemistry) of **BN-9,1-Naph** in direct comparison to the three existing parental BN naphthalenes (**BN-1,2-Naph**, **BN-9,10-Naph**, and **BN-1,9-Naph**) allowed us to establish guiding principles concerning the electronic structure as a function of the position and orientation of the BN unit placement. Furthermore, we demonstrate that BN/CC isosterism in the context of **BN-9,1-Naph** can impact crystal packing to favor a π-stack motif.

The synthesis of **BN-9,1-Naph** commences with the commercially available 2-vinylpyridine **1** that reacts with the *in situ* generated allylboron dichloride[12] to give adduct **2**. Without further purification, compound **2** in the presence of

Received: March 16, 2017
Published: April 19, 2017

DOI: 10.1021/jacs.7b02661
J. Am. Chem. Soc. 2017, 139, 6082−6085

Grubbs' first generation metathesis catalyst produces the ring-closed compound **3** in good yield over two steps. Elimination of HCl from **3** is promoted by triethylamine as the base to furnish the *B*−Cl substituted BN naphthalene derivative **4**. Subsequent addition of lithium aluminum hydride gives the parent **BN-9,1-Naph**. It is worth noting that **BN-9,1-Naph**, like its isomers **BN-1,2-Naph**, **BN-9,10-Naph**, and **BN-1,9-Naph**, has an odor akin to that of naphthalene.

Unfortunately, the crystal structure of the parent **BN-9,1-Naph** is disordered. However, single-crystal X-ray analysis of fluorine-substituted **7F-BN-9,1-Naph** (prepared using the same synthetic route, Scheme 1) unambiguously established the

Scheme 1. Synthesis of BN-9,1-Naph and 7F-BN-9,1-Naph

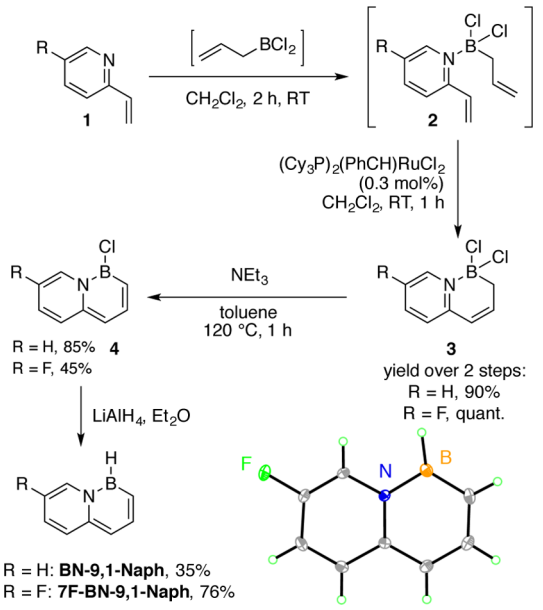

connectivity of the **BN-9,1-Naph** core (Scheme 1, bottom right ORTEP illustration). Analysis of the crystal packing of **BN-9,1-Naph** reveals a "herringbone" motif (Figure 2a) much like its all-carbon analogue, naphthalene,[13] and also like its isomers **BN-1,2-Naph**,[14] **BN-9,10-Naph**,[15] and **BN-1,9-Naph**.[8b] On the other hand, **7F-BN-9,1-Naph** adopts a packing motif featuring face-to-face π-stacks (Figure 2b). The packing motif of this polymorph of **7F-BN-9,1-Naph** contrasts that of its all-carbon isostere 2-fluoronaphthalene, which instead adopts the herringbone motif.[16] Thus, the unique packing is a direct result of BN/CC isosterism. The average distance between layers is 3.36 Å, which is consistent with π-stacking interactions.[17]

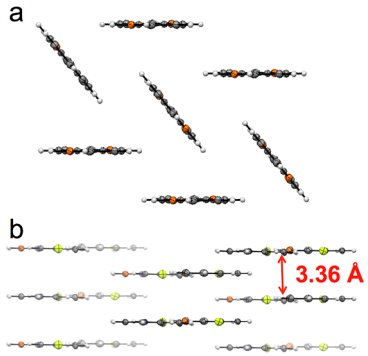

Figure 2. Crystal packing of (a) parent **BN-9,1-Naph**, also representative of the packing of parent **BN-1,2-Naph**, **BN-9,10-Naph**, **BN-1,9-Naph**; (b) fluorinated **7F-BN-9,1-Naph**. Thermal ellipsoids are drawn at the 50% probability level.

We characterized the electronic structure of **BN-9,1-Naph** by UV-photoelectron spectroscopy (UV-PES) along with the three currently known parental BN naphthalenes **BN-1,9-Naph**, **BN-9,10-Naph**,[18] and **BN-1,2-Naph** (Figure 3).[19] We have

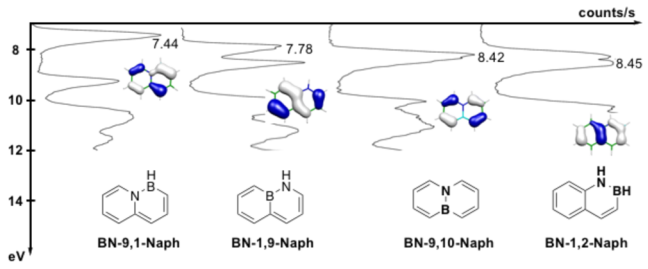

Figure 3. UV-PE spectra and the first ionization potential of parental BN naphthalenes **BN-9,1-Naph**, **BN-1,9-Naph**, **BN-9,10-Naph**, and **BN-1,2-Naph**.

previously used this technique in concert with DFT calculations to match experimentally determined ionization energies with occupied molecular orbitals of BN heterocycles.[6,7,20] As can be seen from Figure 3, not only do the HOMO orbital shapes of these BN naphthalene isomers differ from one another, but so do their corresponding HOMO energy levels. The trend with respect to the HOMO energy levels is as follows: **BN-9,1-Naph** (−7.44 eV) > **BN-1,9-Naph** (−7.78 eV) > **BN-9,10-Naph** (−8.42 eV) > **BN-1,2-Naph** (−8.45 eV).

To evaluate the LUMO energy levels of these BN naphthalene isomers, we conducted cyclic voltammetry experiments.[21] Each BN naphthalene exhibited irreversible reduction; thus, the cathodic peak potentials for these compounds were used for comparison. Ranked by increasing magnitude of cathodic peak potential (E_{pc} vs Fc/Fc^+ in $MeCN/Bu_4NPF_6$) are **BN-1,9-Naph** (−2.57 V), **BN-9,1-Naph** (−2.82 V), **BN-1,2-Naph** (−2.95 V), **BN-9,10-Naph** (−3.34 V), with **BN-1,9-Naph** being the compound that is easiest to reduce and thus featuring the lowest-energy LUMO among the BN naphthalenes that we have investigated. The experimentally determined electrochemical data for the BN naphthalene series are consistent with the LUMO energy and electron affinity trends predicted by the calculations (see Figure 4 and Table S3 in the Supporting Information).

We then turned our attention to UV−vis absorption spectroscopy. Figure 5 shows the UV−vis spectra of **BN-9,10-Naph**, **BN-1,2-Naph**, **BN-1,9-Naph**, and **BN-9,1-Naph** along with a table summarizing key parameters associated with their frontier orbital energies. Apparent from Figure 5 is that the two orientational isomers **BN-1,9-Naph** (orange trace) and **BN-9,1-Naph** (red trace) exhibit more similar electronic transitions than other BN naphthalene counterparts. Their experimentally determined optical HOMO−LUMO gaps[23] are very similar to each other. The trend for the optical HOMO−LUMO gap (**BN-9,10-Naph** > **BN-1,2-Naph** > **BN-1,9-Naph** ~ **BN-9,1-Naph**) is consistent with the trend predicted by TD-DFT calculations (see Table in Figure 5).

Based on our data (UV-PES, CV, UV−visible absorption, calculations), the following electronic structure guiding principles became apparent. Isomeric BN naphthalenes in

DOI: 10.1021/jacs.7b02661
J. Am. Chem. Soc. 2017, 139, 6082−6085

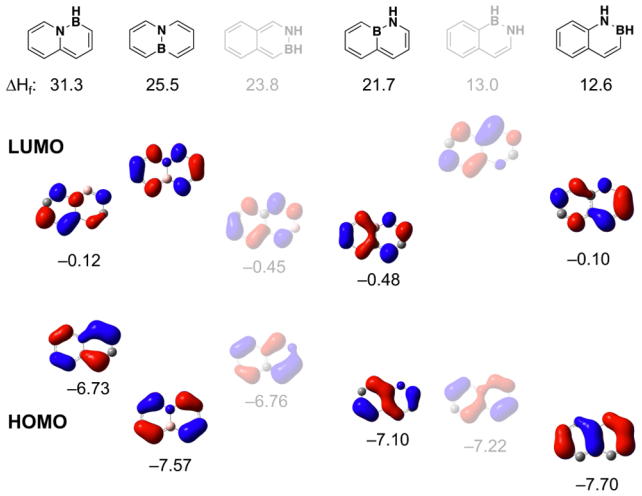

Figure 4. Calculated [CAM-B3LYP/6-311G(d,p)] Kohn−Sham HOMO and LUMO energies (in eV) and calculated (G3MP2) heats of formation ΔH_f (in kcal/mol) for BN naphthalenes. The calculated LUMO energies for **BN-9,10-Naph** and **2,1-BN-Naph** are >0 eV and thus are not shown.[22]

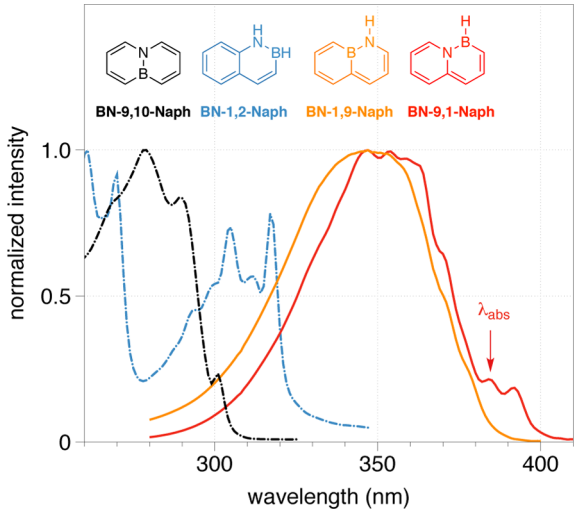

	λ_{abs} (nm)	Optical HOMO-LUMO gap (eV)	Calcd TD-DFT transition (eV)	HOMO Energy exp. (eV)	E_{pc} (V vs. Fc/Fc$^+$)
BN-9,10-Naph	279	4.13	4.96	−8.42	−3.34
BN-1,2-Naph	317	3.85	4.72	−8.45	−2.95
BN-1,9-Naph	347	3.21	4.05	−7.78	−2.57
BN-9,1-Naph	384	3.10	3.98	−7.44	−2.82

Figure 5. UV−visible absorption spectra of BN naphthalenes (cyclohexane solvent) with key optoelectronic parameters.[24] Calculated energies were obtained using TD-DFT at the CAM-B3LYP/6-311G(d,p) level. E_{pc} values were collected in 0.1 M MeCN/Bu_4NPF_6 at 150 mV/s.

which the B−N bond remains in the same *location* with respect to the acene topology but is inverted in *orientation* (i.e., orientational isomers: **BN-1,9-Naph**/**BN-9,1-Naph** and **BN-1,2-Naph**/**BN-2,1-Naph**) have very similar HOMO−LUMO gaps (Figure 6). Furthermore, between each pair of orientational isomers, the more thermodynamically stable compound (with the smaller ΔH_f value) has the more stable HOMO energy of the two (see Figure 4). Calculations for the BN anthracene series (see Supporting Information) suggest that

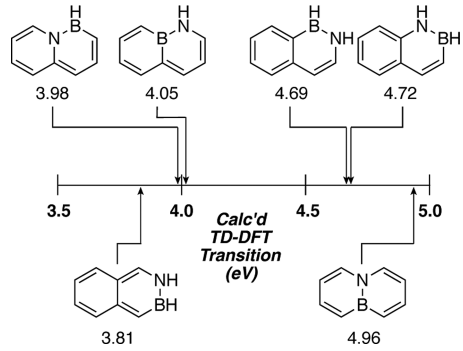

Figure 6. TD-DFT excitation energies associated with the HOMO−LUMO transition of BN naphthalenes calculated at the CAM-B3LYP/6-311G(d,p) level.

these guiding principles may be general for higher BN acenes as well.

In summary, we have developed a simple four-step synthesis to the least stable isomer of the parental BN naphthalene series, **BN-9,1-Naph**. The synthetic access to **BN-9,1-Naph** in combination with three other parental BN naphthalene isomers enabled the most systematic comparative electronic structure analysis for BN isosteres of PAHs to date, which we have achieved using a combined experimental (UV-PES, CV, UV−vis) and theoretical/computational approach. Two predictive guiding principles can be established from our work: (1) Orientational BN isomers have similar HOMO−LUMO gaps. (2) For each pair of orientational BN isomers, the more thermodynamically stable compound has the more stable HOMO energy. Furthermore, we demonstrated in the context of the fluorinated **7F-BN-9,1-Naph** that BN/CC isosterism can influence the crystal packing, resulting in a face-to-face π-stacking motif for **7F-BN-9,1-Naph** vs a herringbone motif for its carbonaceous isostere 2-fluoronaphthalene. The established trends in this work may be general for other BN acenes. Thus, our findings should aid in further targeted syntheses of BN acenes for optoelectronic applications.

■ ASSOCIATED CONTENT

Supporting Information

The Supporting Information is available free of charge on the ACS Publications website at DOI: 10.1021/jacs.7b02661.

Experimental, computational, and crystallographic information; complete Gaussian 09 reference (PDF)
BN-9,1-Naph crystal structure (CIF)
7F-BN-9,1-Naph crystal structure (CIF)

■ AUTHOR INFORMATION

Corresponding Authors

*shihyuan.liu@bc.edu
*anna.chrostowska@univ-pau.fr

ORCID

Zhiqiang Liu: 0000-0001-7863-1759
David A. Dixon: 0000-0002-9492-0056
Shih-Yuan Liu: 0000-0003-3148-9147

Present Address

⊥State Key Laboratory of Crystal Materials, Shandong University, Jinan 250100, China.

Author Contributions

‖Z.L. and J.S.A.I contributed equally.

DOI: 10.1021/jacs.7b02661
J. Am. Chem. Soc. 2017, 139, 6082−6085

Notes

The authors declare no competing financial interest.

■ ACKNOWLEDGMENTS

This research was supported by the National Science Foundation (CHE-1561153). We thank Dr. Alec N. Brown for providing precursors for **BN-1,9-Naph**. J.S.A.I. thanks the LaMattina Family Graduate Fellowship in Chemical Synthesis for support. The UA work was supported by the Chemical Sciences, Geosciences and Biosciences Division, Office of Basic Energy Sciences, U.S. Department of Energy (DOE) Catalysis Center Program. D.A.D. also thanks the Robert Ramsay Chair Fund of The University of Alabama for support. A.C. thanks A. Mazière for preliminary work and P. Baylère for technical assistance.

■ REFERENCES

(1) For an overview, see: (a) Liu, Z.; Marder, T. B. *Angew. Chem., Int. Ed.* **2008**, *47*, 242−244. (b) Bosdet, M. J. D.; Piers, W. E. *Can. J. Chem.* **2009**, *87*, 8−29. (c) Campbell, P. G.; Marwitz, A. J. V.; Liu, S.-Y. *Angew. Chem., Int. Ed.* **2012**, *51*, 6074−6092.

(2) For an overview, see: Wang, X.-Y.; Wang, J.-Y.; Pei, J. *Chem. - Eur. J.* **2015**, *21*, 3528−3539.

(3) For select examples, see: (a) Yang, D.-T.; Mellerup, S. K.; Peng, J.-B.; Wang, X.; Li, Q.-S.; Wang, S. *J. Am. Chem. Soc.* **2016**, *138*, 11513−11516. (b) Davies, G. H. M.; Zhou, Z.-Z.; Jouffroy, M.; Molander, G. A. *J. Org. Chem.* **2017**, *82*, 549−555. (c) Huang, H.; Pan, Z.; Cui, C. *Chem. Commun.* **2016**, *52*, 4227−4230. (d) Neue, B.; Araneda, J. F.; Piers, W. E.; Parvez, M. *Angew. Chem., Int. Ed.* **2013**, *52*, 9966−9969. (e) Rohr, A. D.; Kampf, J. W.; Ashe, A. J., III *Organometallics* **2014**, *33*, 1318−1321. (f) Wang, X.-Y.; Lin, H.-R.; Lei, T.; Yang, D.-C.; Zhuang, F.-D.; Wang, J.-Y.; Yuan, S.-C.; Pei, J. *Angew. Chem., Int. Ed.* **2013**, *52*, 3117−3120. (g) Zhuang, F.-D.; Han, J.-M.; Tang, S.; Yang, J.-H.; Chen, Q.-R.; Wang, J.-Y.; Pei, J. *Organometallics* In Press. DOI: 10.1021/acs.organomet.6b00811. (h) Hatakeyama, T.; Hashimoto, S.; Seki, S.; Nakamura, M. *J. Am. Chem. Soc.* **2011**, *133*, 18614−18617. (i) Hashimoto, S.; Ikuta, T.; Shiren, K.; Nakatsuka, S.; Ni, J.; Nakamura, M.; Hatakeyama, T. *Chem. Mater.* **2014**, *26*, 6265−6271. (j) Wang, X.; Zhang, F.; Liu, J.; Tang, R.; Fu, Y.; Wu, D.; Xu, Q.; Zhuang, X.; He, G.; Feng, X. *Org. Lett.* **2013**, *15*, 5714−5717. (k) Zhang, W.; Zhang, F.; Tang, R.; Fu, Y.; Wang, X.; Zhuang, X.; He, G.; Feng, X. *Org. Lett.* **2016**, *18*, 3618−3621.

(4) For examples with limited comparisons, see: (a) Dewar, M. J. S.; Poesche, W. H. *J. Am. Chem. Soc.* **1963**, *85*, 2253−2256. (b) Bosdet, M. J. D.; Jaska, C. A.; Piers, W. E.; Sorensen, T. S.; Parvez, M. *Org. Lett.* **2007**, *9*, 1395−1398. (c) Wang, X.-Y.; Narita, A.; Feng, X.; Müllen, K. *J. Am. Chem. Soc.* **2015**, *137*, 7668−7671. (d) Michl, J.; Jones, R. *Collect. Czech. Chem. Commun.* **1971**, *36*, 1233−1247. (e) Wang, S.; Yang, D.-T.; Lu, J.; Shimogawa, H.; Gong, S.; Wang, X.; Mellerup, S. K.; Wakamiya, A.; Chang, Y.-L.; Yang, C.; Lu, Z.-H. *Angew. Chem., Int. Ed.* **2015**, *54*, 15074−15078.

(5) Morgan, M. M.; Piers, W. E. *Dalton Trans.* **2016**, *45*, 5920−5924.

(6) Chrostowska, A.; Xu, S.; Lamm, A. N.; Mazière, A.; Weber, C. D.; Dargelos, A.; Baylère, P.; Graciaa, A.; Liu, S.-Y. *J. Am. Chem. Soc.* **2012**, *134*, 10279−10285.

(7) Ishibashi, J. S. A.; Marshall, J. L.; Mazière, A.; Lovinger, G. J.; Li, B.; Zakharov, L. N.; Dargelos, A.; Graciaa, A.; Chrostowska, A.; Liu, S. *J. Am. Chem. Soc.* **2014**, *136*, 15414−15421.

(8) (a) Marwitz, A. J. V; Matus, M. H.; Zakharov, L. N.; Dixon, D. A.; Liu, S.-Y. *Angew. Chem., Int. Ed.* **2009**, *48*, 973−977. (b) Brown, A. N.; Li, B.; Liu, S.-Y. *J. Am. Chem. Soc.* **2015**, *137*, 8932−8935.

(9) Dewar, M. J. S.; Dietz, R. *J. Chem. Soc.* **1959**, 2728−2730.

(10) Dewar introduced non-standard numbering of the naphthalene core for this species: Dewar, M. J. S.; Gleicher, G. J.; Robinson, B. P. *J. Am. Chem. Soc.* **1964**, *86*, 5698−5699.

(11) Liu, X.; Wu, P.; Li, J.; Cui, C. *J. Org. Chem.* **2015**, *80*, 3737−3744.

(12) Bubnov, Y. N.; Kuznetsov, N. Y.; Pastukhov, F. V.; Kublitsky, V. V. *Eur. J. Org. Chem.* **2005**, 4633−4639.

(13) Oddershede, J.; Larsen, S. *J. Phys. Chem. A* **2004**, *108*, 1057−1063.

(14) Pan, J.; Kampf, J. W.; Ashe, A. J., III *Organometallics* **2009**, *28*, 506−511.

(15) Fang, X.; Yang, H.; Kampf, J. W.; Banaszak Holl, M. M.; Ashe, A. J., III *Organometallics* **2006**, *25*, 513−518.

(16) Chanh, N. B.; Haget-Bouillaud, Y. *Acta Crystallogr., Sect. B: Struct. Crystallogr. Cryst. Chem.* **1972**, *28*, 3400−3404.

(17) Curtis, M. D.; Cao, J.; Kampf, J. W. *J. Am. Chem. Soc.* **2004**, *126*, 4318−28.

(18) Dewar reported a photoelectron spectrum of **BN-9,10-Naph**: Davis, F. A.; Dewar, M. J. S.; Jones, R.; Worley, S. D. *J. Am. Chem. Soc.* **1968**, *90*, 706−708. We report here a higher-resolution UV-PE spectrum collected with our own equipment for consistency

(19) See Supporting Information for experimental details.

(20) Chrostowska, A.; Xu, S.; Mazière, A.; Boknevitz, K.; Li, B.; Abbey, E. R.; Dargelos, A.; Graciaa, A.; Liu, S.-Y. *J. Am. Chem. Soc.* **2014**, *136*, 11813−11820.

(21) See Supporting Information for cyclic voltammograms and experimental details.

(22) LUMO energies >0 eV have no physical meaning.

(23) The optical HOMO−LUMO gap was estimated using the intersection of the *x*-axis by the line tangent to the onset of the absorption peak associated with the HOMO−LUMO transition. TD-DFT calculations (see Supporting Information) have been used to assign the peaks associated with the HOMO−LUMO transition.

(24) λ_{abs} is defined here as the absorption wavelength associated with the HOMO−LUMO transition.

DOI: 10.1021/jacs.7b02661
J. Am. Chem. Soc. 2017, 139, 6082−6085